Exploiting Asynchronous Invariance for Resistant Encrypted Watermark Embedded in Radon Field

Dhekra ESSAIDANI, Hassene SEDDIK, Ezzedine BEN BRAIEK
Products Research Centre (CEREP) ESSTT
5 Av. Taha Hussein, 1008, Tunis
Tunisia
dhekraessaidani89@gmail.com, {seddik_hassene, ebenbraiek}@yahoo.fr

ABSTRACT: *The rapid evolution of technology and its applications have created the need for new techniques for copyright protection and data owner identification. Many researches are proposed to establish a potential solution to protect the ownership rights. In the last years, various watermarking techniques have been proposed to protect digital data online. This work presents a watermarking approach based on Radon Transform applied to RGB color image. The simulation results show that the proposed method presents a higher robustness against asynchronous attacks. Also, the comparative study with other recent techniques proved the efficiency of the proposed approach.*

Keywords: Discrete Radon Transform, Color Image Watermarking, Geometric Attacks, Asynchrony Attacks, Robustness, Radial Integration Transform (RIT), Circular Integration Transform (CIT)

Received: 29 June 2013, Revised 2 August 2013, Accepted 11 August 2013

1. Introduction

The evolution of technology facilitates the data transfer but it also increases the ability of hacking such information. Therefore, several techniques are proposed to protect data online. On the other side, its applications present always errors and limitations. Encryption and Steganography are the two developed techniques to protect online information. In 1992, the research suggested using the watermarking technique in data protection. Nowadays, watermarking represents an important search subject. The core idea of watermarking involves integrating a message into a digital content. This last covers the information to be transmitted in a holder in a way to be invisible and correctly reversible (an algorithm allows the exact extraction of the embedded watermark). Its algorithm requires equilibrium between these three constraints: imperceptibility, robustness and embedding capacity [3].

The attack process represents the first danger to watermarking image. Therefore, it can mislead the watermark detector. A practical digital watermarking scheme must be resistant to a variety of possible attacks [10]. In the order, various watermarking schemes are proposed for the digital multimedia protection. Most of the schemes perform on the spatial domain where the watermarking techniques directly modify the intensities of selected pixels [4]. Also, several schemes perform on the transformation domain where the watermarking algorithm modifies the selected transformed coefficients. The literature has defined different transform domains used for watermarking image such as: Fourier-Mellin Transform, Discrete Cosine Transform (DCT), the Discrete Fourier Transform (DFT), the Discrete Wavelet Transform and the Complex Wavelet Transform (CWT) [2].

Several watermarking algorithms using color image are developed to protect data. In [8, 9 and 5], authors have proposed two different schemes for copyright protection of color image based on SVD in DWT domain for hiding watermark in full frequency band of color images. On the other hand, researches show that the resistivity of watermarking schemes against geometric attacks remains low [6]. D. Simitopoulos, DE. Koutsonanos and M.G.Strintzis proposed a "*Robust Image Watermarking Based on Generalized Radon Transformations*" [7]. Other researches combine the Radon field with other field to embed the watermark. In [11], the authors combined the Radon transform and complex moments to create an invariant digital image watermarking against geometric attacks. Also, B. Xiao, J. FengMa and J.TaoCui proposed a new method to resist against global geometric transforms. They combined the Radon field with the pseudo-Fourier–Mellin transform to embed the watermark. This combination is noted Radon and pseudo-Fourier–Mellin invariants (RPFMI) [10].

In order to resist against geometrics attacks, we proposed in this work a new watermarking algorithm based on RGB color image. Our approach selects specific coefficients in Radon field to embed watermark in the media. This paper is organized as follows: Section 2 presents an overview of Radon Transform (RT). Section 3 details our watermarking method. In section 4, we study the robustness of this technique against different STIRMARK attacks. A study of the watermarked image distortions before and after different attacks is also presented. In section 5 a mathematical study is developed to explain the resistance of the proposed method and prove the results found.

2. Mathematical Recall of Discrete Radon Transformation

In 1917, J. Radon, Austrian mathematician, defined the theory of Radon Transform. He proved the possibility of reconstructing a function of a space from knowledge of its integration along the hyper-plans in the same space. This theory establishes the reversibility of the transformed Radon and the transition between the native function space and the Radon space, or the space of projections. The generalized Radon transform of a function $f(x, y)$ is defined at [1] by the following equation:

$$R(\rho, \theta) = \int_{-\infty}^{+\infty} \int_{-\infty}^{+\infty} f(x, y)\, \delta(x\cos\theta, y\sin\theta - \rho)\, dxdy \tag{1}$$

Where ρ represents the perpendicular distance of a straight line from the origin, and θ represents the angle between the distance vector and the *x*-axis.

The literature proposed two categories of Radon transform. The first one based on Radial Integration Transform **(RIT).** The second one based on the Circular Integration Transform (**CIT**).

In image processing, the Radon Transform represents a collection of projections along various directions. The discrete Radial Integration Transform of $I(x, y)$ is defined at [6] by the following equation:

$$R(t\Delta\theta) = \frac{1}{J}\sum_{j=1}^{J} I(x_0 + t\Delta s.\cos(t\Delta\theta), y_0 + j\Delta s.\sin(t\Delta\theta)) \tag{2}$$

The discrete Circular Integration Transform of $I(x, y)$ is defined by the following equation [6]:

$$C(k\Delta\rho) = \frac{1}{T}\sum_{t=1}^{T} I(x_0 + k.\Delta\rho.\cos(t.\Delta\theta), y_0 + k.\Delta\rho.\sin(t.\Delta\theta)) \tag{3}$$

Where $\Delta\theta$ represents the angular variation step, Δs is the scaling step, $k\Delta\rho$ represents the radius of the smallest circle that encircles the image, J represents the number of samples on the radius with orientation θ, $t = 1,\ldots..., \frac{360}{\Delta\theta}$ and $k = 1,\ldots..., \frac{\rho_{\max}}{\Delta\rho}$

The Radon transform of the image $I(x, y)$ defined by its size $[M \quad N]$ generate a matrix $R(\rho, \theta)$ witch real coefficient and its size is equal to $[R \quad T]$:

$$\begin{cases} R = \sqrt{N^2 + M^2 + 1} \\ T = \dfrac{\theta_{\max}}{\Delta\theta} \end{cases} \tag{4}$$

3. Proposed Watermarking Method

Due to the expansion of the projected image matrix from its size [$M\ N$] to [$R\ T$], this field allows a higher amount of the embedded data. In fact the DRT increases the size of the transformed image (see equation 4). The proposed method consists to embed the watermark in the selected coefficients from the radon matrix. These coefficients defined the area of the maxima radon coefficients. It holds the maximal energy of the transformed image. This is done for three essentials reasons:

- The first one, these coefficients are set on the integral line of projection. They will be well recovered from the inverse radon transform.
- Secondly, they contain the most important details of the original images. Consequently, they are the most adapted to code in a watermark with better imperceptibility.
- Their high values permit to embed and cover the binary coefficients of the watermark without any perceptual degradation of the watermarked image.

3.1 The Proposed algorithm

In the following, we will note by W_o the original watermark. W is the encrypted watermark to embed. W' represents the recovered encrypted watermark. W_o' is the recovered and decrypted watermark, I the Original image (support), Rb the blue matrix in Radon field. Rb' is the watermarked blue matrix in Radon field. (x, y) is the spatial coordinates of the original image, (ρ, θ) is the coordinates of the original image in radon field. k and l are the coded bits used to embed and to extract the watermark. [$M\ N$] is the Size of the original image. [$M_w N_w$] represents the size of the original watermark and G is the embedding strength.

3.1.1Watermarking algorithm

The main concept of the watermark embedding process is shown by the following diagram:

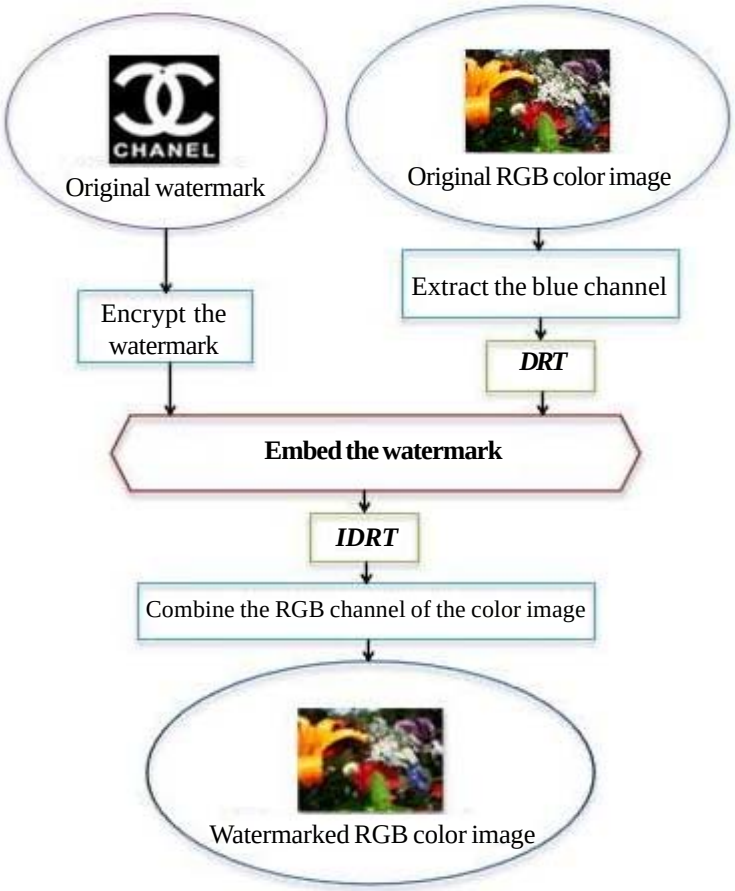

Figure 1. Watermarking algorithm

The proposed algorithm is detailed by the following steps:

• **Step 1: T**he watermark W is transformed into a one dimensional vector. Twenty permutations are applied on this vector to create the encrypted watermark as presented by the following steps and equations:

1. Decompose the watermark in N equal blocs: B_i

$$W(N) = \{B_1, B_2, ..., B_N\} \tag{5}$$

Where $i = \{1, 2, ..N\}$

2. Permute each bloc by using the two followings equations:

$$P_{s=1}(B_1, ..., B_N) = W : \{B_{N/2}, ...B_1, B_N, ..., B_{((N/2)+1)}\} \tag{6}$$

After each permutation, the resulting vector is decomposed in to N equal blocs B_i whereWhere $i = \{1, 2, ..N\}$and the next permutation is applied increasing the step of S until the maximum permutation numbers is reached.

3. The permutation corresponding to $S = 2$ is illustrated by the following equation:

$$P_{s=2}(B_1, ..., B_N) = P_{s=1}\{B_N, ...B_{(N/2)}, B_N, ..., B_{((N/2)+1)}\} \tag{7}$$

4. Permute iteratively the set of blockstimes, for $\alpha = 3 \rightarrow S_{\max}$, the permutations given by the following equation:

$$\underset{\alpha = 3 \rightarrow S_{max}}{P_{s=\alpha}(B_1, ..., B_N)} = P_{s=\alpha-1}\{B_N, ...B_{(N/2)}, B_1, ..., B_{((N/2)+1)}\} \tag{8}$$

5. We fixed $S_{\max} = 20$ and the encrypted message is obtained after 20 permutations. It is defined as follows:

$$W(k) = P_{s=20}(k) \tag{9}$$

• **Step 2:** In this step, we applied the Radial Integration Transform with integration path $\Delta\theta = 1°$ and $\Delta\rho = 1$ *pixels* only to the blue component of the color image. Then, we selected the $M_w \times N_w$ higher coefficients from *Rb*. For this reason, we transformed the image matrix into a vector V in downward order by the following equation:

$$\underset{[M_\rho N_\theta]}{Rb(\rho, \theta)} \rightarrow \underset{M_\rho * N_\theta}{V}(k) \tag{10}$$

Next, we selected the threshold λ defined by its position $(M_w \times N_w)$ in the defined vector V. This instruction is defined by the following equation:

$$\lambda = V(M_w \times N_w) \tag{11}$$

This threshold is used for selected the coefficients for coding the watermark. This step is defined as follows:

$$\underset{E:1 \rightarrow M_w \times N_w}{R_E(\rho, \theta)} \geq \lambda \tag{12}$$

So, these coefficients represent the $M_w \times N_w$ first coefficients in the vector V:

$$\underset{E:1 \rightarrow M_w \times N_w}{R_E(\rho, \theta)} = \underset{l:1 \rightarrow M_w \times N_w}{V(l)} \tag{13}$$

• **Step 3:** The embedding process is described by the following diagram and equation 13.

$$Rb(\rho, \theta) \rightarrow Rb(\rho, \theta) + G.W(k) \tag{14}$$

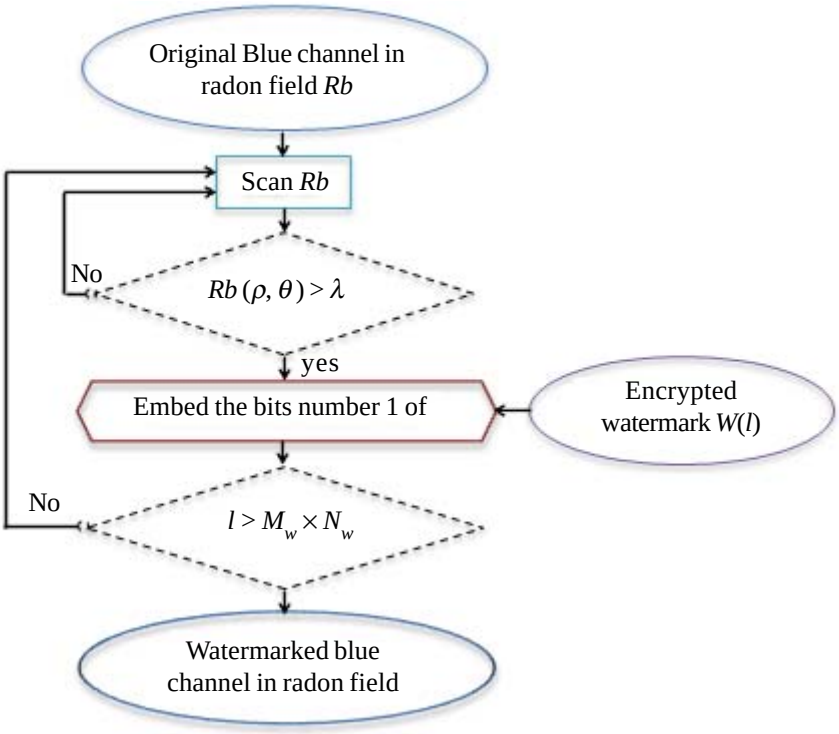

Figure 2. Embedding process

• **Step 4**: We applied the inverse DRT (**IDRT**) to the watermarking blue matrix. We combine the RGB channel of the color image to create the watermarked color image in spatial domain.

3.1.2 Watermark Extraction process

This step of watermarking approach consists to recover the embedded watermark from the media. Its algorithm is detailed by the following algorithm:

In this algorithm, we extract the blue channel from the watermarked image in spatial filed. Then, we applied a radon transform with the same parameter used in the embedding process (step2 paragraph 3.1.1) for the extract channel. This transformation gives the watermarked image in radon field Rb'. The λ' represents the threshold used to select the used coefficient to embed the original watermark. It represents the highest coefficient number ($M_w \times N_w$) in the matrix Rb' (The blue watermarked matrix in Radon domain). For this reason, we transformed the image matrix into a vector V' in downward order using the following equation:

$$\underset{[M_\rho N_\theta]}{Rb'(\rho, \theta)} \rightarrow \underset{M_\rho * N_\theta}{V'(l)} \text{ with } l = \rho \times \theta \tag{15}$$

Next, we selected the threshold λ' defined by its position ($M_w \times N_w$) in the defined vector V'. This instruction is defined by the following equation:

$$\lambda' = V'(M_w \times N_w) \tag{16}$$

The threshold λ' used to define the used coefficients for coding the watermark. These coefficients represents ($M_w \times N_w$) first coefficients in the vector V' verify the two following conditions:

1) It is higher to the threshold λ':

$$\underset{E: 1 \rightarrow [M_W \times N_W]}{Rb'_E(\rho, \theta)} \geq \lambda' \tag{17}$$

2) These coefficients represent the $M_w \times N_w$ first coefficients in the vector V':

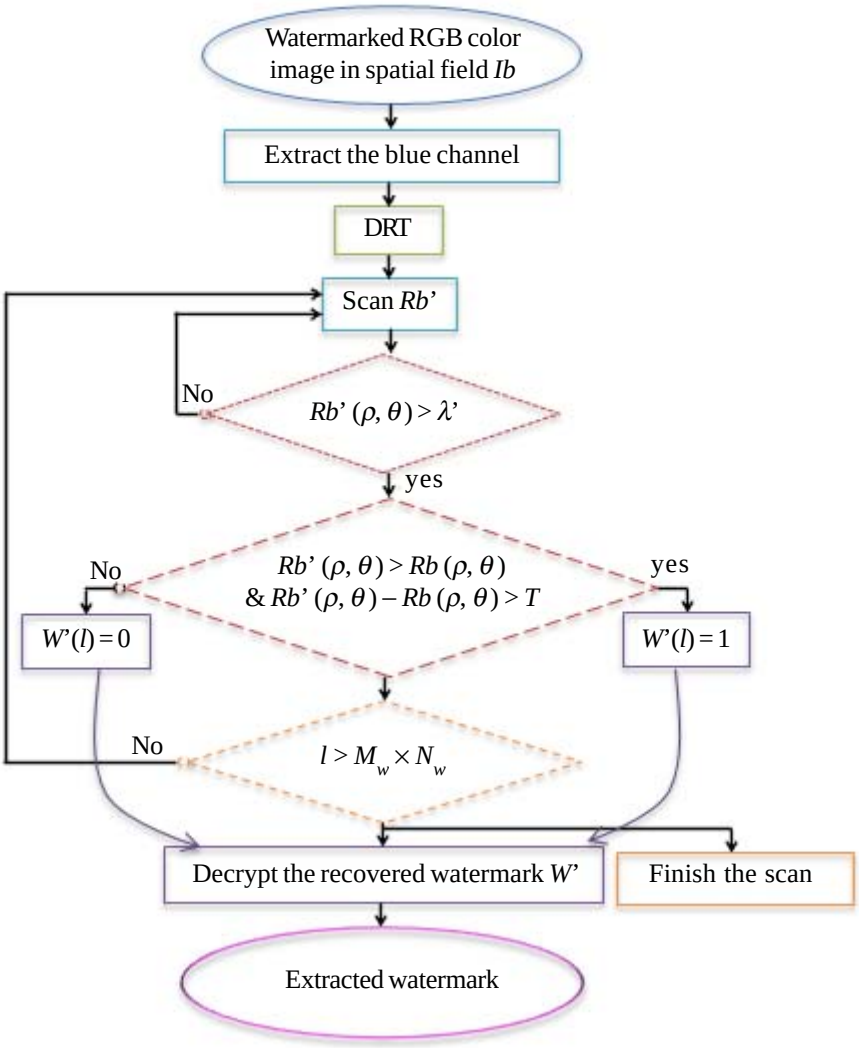

Figure 3. Extraction process

$$R'_{E:1\to M_w\times N_w}(\rho,\theta) = V'_{l:1\to M_w\times N_w}(l) \tag{18}$$

Then, it given T is the selected threshold deciding if the compared bit belongs to the watermark or not. The recovered watermark W' is a one dimensional vector. It is an encrypted watermark. To decrypt it, we used the inverse algorithm used to encrypt the original watermark with the same parameters.

1. Decompose the watermark W' in N' equal blocs B_j where $j = \{1, 2 \ldots N'\}$ ($N' = N$: N is the number of blocs used in equation (7))

$$W'(N') = W' : \{B_1, B_2, \ldots, B_{N'}\} \tag{19}$$

2. The first inverse permutation for $S = 1$ is given by the following equation:

$$P_{S=1}(B_1, \ldots, B_{N'}) = W'\{B_{N'}, B_{N'/2}, \ldots, B_{((N'/2)+1)}\} \tag{20}$$

After each permutation, the resulting vector is decomposed in to N' equal blocs B_j where $j = \{1, 2 \ldots N'\}$ and the next permutation is applied increasing the step of $a$until the maximum permutation numbers is reached.

3. Permute iteratively the set of blocks S times, the permutation corresponding to $S = 2$ be illustrated by the following equation:

$$P_{S=2}(B_1,...,B_{N'}) = P_{S=1}\{B_{N'}, B_{(N'/2)},...,B_{((N'/2)+1)}\} \tag{21}$$

4. For $a = 3 \rightarrow S_{max}$ the permutation is given by the following equation:

$$\underset{a=3\rightarrow S_{max}}{P_{S=a}}(B_1,...,B_{N'}) = P_{S=a-1}\{B_N,..., B_{(N'/2)}, B_1,...,B_{((N'/2)+1)}\} \tag{22}$$

5. The finally recovered watermark is obtained after 20 permutations. It is defined by:

$$W_o^{'}(k) = P_{S=20}(B_1, B_2,...,B_{N'}) \tag{23}$$

It is transformed to a matrix with size equal to $(M_w \times N_w)$. So, it represents the recovered watermark $W_o^{'}$.

3.2 Simulation results

To evaluate the performance of the proposed watermarking scheme, we used a base data composed with 100 watermarks. Different tests are given results simulate of the present results for the used watermark at (Figure 7). In this paper, we represents the result of the color image "*Lena*" (see Figure 9). Its size is equal to (256×256). The size of the watermark Figure 7) is equal to (32×32). To apply the **DRT** to original image, we used $\theta_{max} = 2\pi$ and the path $\Delta\theta = 1^{\circ}$. The system origin of projection is (x_0, y_0) and the path scaling integration is $\Delta\rho = 1$ *pixel*.

The similitude rate between the extracted watermark and the original watermark is continuously computed to test the robustness of this approach. This is done by the normalized correlation presented by the following figure:

$$NC = \frac{\sum_{i=1}^{M_q}\sum_{1}^{N_q} Wo\, Wo'}{\sqrt{\left[\sum_{1}^{M_q}\left(\sum_{1}^{N_q} Wo^2\right)\sum_{1}^{M_q}\left(\sum_{1}^{N_q} Wo'^2\right)\right]}} \tag{24}$$

On the other hand, the imperceptibility of the embedded watermark is a constraint that must be respected. A PSNR measure is computed (see equation 16 and 17) after each embedding process with respect to the gain factor used. A threshold of 37 dB is fixed to verify if some distortions begin to appear on the watermarked image in addition to a psycho-visual decision.

$$PSNR = 10 \log 10 \frac{d^2}{MSE} \tag{25}$$

Where d represents the maximal gray scale and MSE is calculated by the following equation:

$$MSE = \frac{1}{N_q \times M_q}\sum_{i=1}^{N_q \times M_q}(Wo - Wo')^2 \tag{26}$$

An example of an original and a watermarked image is illustrated by the following figures:

Figure 4. Original image

Figure 5. Watermarked image

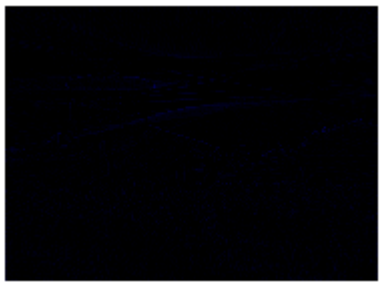

Figure 6. Spatial difference between the original and watermarked image

Figure 7. Original Watermark

Figure 8. Encrypted Watermark

Figure 9. Recovered Watermark

The **PSNR** value corresponding to a gain factor G = 1000 is **PSNR = 38.68 dB** between the original and the watermarked color image (Figure. 4 and figure. 5). Also, it generates a **normalized correlation** between original and an extracted watermark is **correlation = 1**(Figure. 7 and figure. 9). The correlation remains equal to 1 for **200** embedding tests for different watermark size and forma. So, this algorithm detects correctly the embedded watermark. Figure 6 shows also the difference Figure 6 shows the spatial difference between the original and the watermarked image. It is represented by blue segments or/and lines spread over the image because the insertion process is doing in the blue matrix of RGB component. It represents the inverse radon transform of the used coefficient in watermark embedding process. We noted that these coefficients represent the most energy area of the transformed image. It defined its edge.

To study the robustness of the proposed approach, different types of attacks are applied to the watermarking image. The correlation between the recovered and original watermark are presented in the following tables. The above figure illustrates the set of coefficients in the radon matrix holding the embedded watermark.

STIRMARK ATTACKS	**Correlation**
Conv_2	1
Median_3	0.9908
Median_5	0.9588
PSNR_0	0.9512
PSNR_50	1
Noise_20	0.9393
Noise_40	0.8945
JPEG_50	0.7666
JPEG_70	0.9979
JPEG_80	1

Table 1. Resistance of the Poposted Method Against the Common Image Processing Attacks

sSTIRMARKATTACKS	Correlation
RESC_90	1
RESC_75	0.9930
RNDDIST_1	1
LATESTRNDDIST	1
RML_10	1
RML_40	0.9978
AFFINE_1	1
AFFINE_8	0.9875
ROT_5	1
ROT_0.75	0.9739
ROT_1	0.9987
ROTCROP_0.5	1
ROTCROP_-1	0.9996
ROTSCALE_-0.25	1
ROTSCALE_0.5	1
ROTSCALE_1	1

Table 2. Resistance of the Poposed Approach Against Asynchrony Attacks

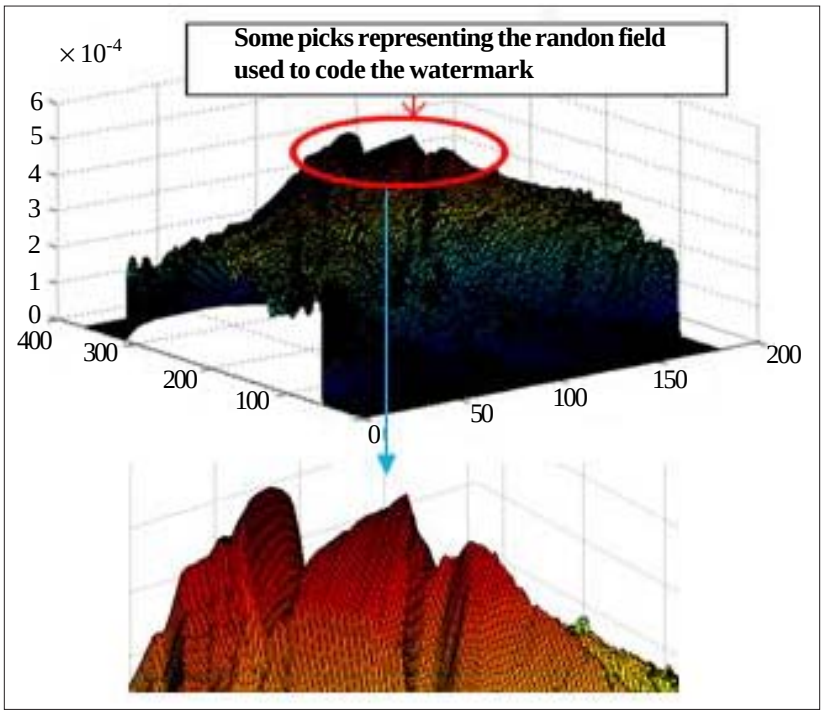

Figure 10. The used coefficients to embed watermark in Radon field

This table shows the effectiveness of the proposed method to resist against different STIRMARK attacks. We note that the resistivity of the proposed approach against geometric attacks is better than that against the synchronous attacks. This efficiency is related to the properties of the Discreet Radon Transform. Also, the effectiveness of the proposed method to resist against common image processing attacks is related to an accurate selection of the coefficients which are/and selected from the image in Radon field. The highest coefficients in the Radon field contain the significant information of the original image that allows to be withstanding against common image processing attacks. Well, these coefficients are located and set on the line of projection. They are also used in the transformed Radon that allows the resilience against the geometrical attacks. This robustness is proved mathematically in the following section.

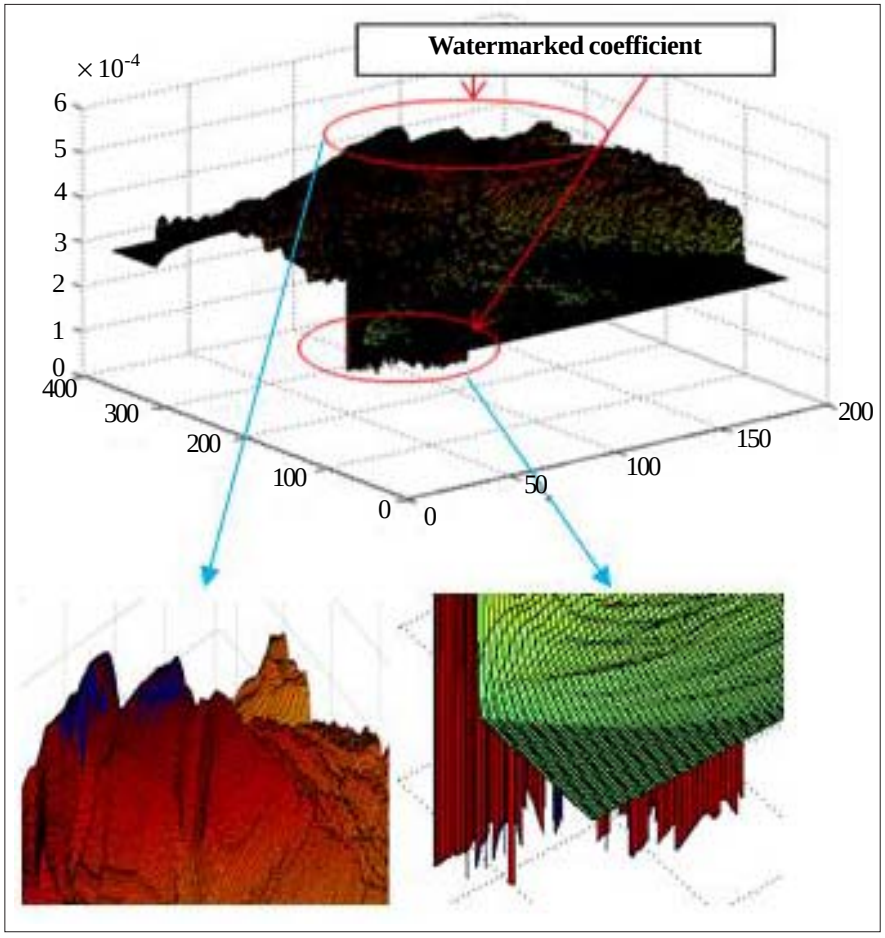

Figure 11. Watermarked image in Radon field

4. Justifying Robustness Gainst Asynchronous Attacks

In this section, we will detail why the Radon Transform resists against the geometrics attacks. This is done through the mathematical characteristics of this transform

4.1 Radon transform presentation

The robustness of the proposed approach and its resistance against asynchronous attacks can be justified only if we prove mathematically that the radon transform is against geometric transforms. In addition this transform has to be entirely reversible and conservative. In the case it is almost conservative, we have a loss of data in the process of applying the DRT and the inverse DRT "DRT^{-1}". This almost conservatively and consequently the data loss must not affect in any way the perceptibility of the watermarked image. All these constraints must be tested and proved. Given an image $I(x, y)$ defined at $\Re_+^2$. $R(\rho, \theta)$ represents its radon projection at $\Re_+^2$. (x, y) and (ρ, θ) represent coordinates of the image in spatial and Radon domain respectively. $[M\ N]$ and $[N_\rho\ N_\theta]$ represent respectively the size of the image in spatial and Radon field. We noted the **D**iscrete **R**adon **T**ransform by

DRT. The invariance faces to the following geometric transforms have to be proved.

4.1.1 Linearity

Given $J(x, y) = K\,I(x, y)$.Where K is a constant. The DRT of $J(x, y)$ gives the following relation:

$$DRT[J(x,y)] = R_1(\rho, \theta) \tag{27}$$

Where :

$$\frac{R_1(\rho, \theta)}{R(\rho, \theta)} = K' \tag{28}$$

Or $K' = K + \Delta K$ Through different tests we find that

$$\Delta K << K \text{ so } K' \cong K \tag{29}$$

Do:

$$R_1(\rho, \theta) = KR(\rho, \theta) \tag{30}$$

So:

$$DRT[J(x,y)] = K\,DRT[I(x,y)] \tag{31}$$

Similarly, we define the following relationship:

If:

$$J(x,y) = K1I1(x,y) + K2W(x,y) \tag{32}$$

The Radon Transformation of J gives the following results:

$$DRT[J(x,y)] = K1\,DRT[I1(x,y)] + K2\,DRT[W(x,y)] \tag{33}$$

Where $[I1(x, y)]$ and $[W(x, y)]$ are two image defined in spatial field and $K1$, K*2* are two constants.

This relation proves that the DRT is linearly invariant.

4.1.2 Scaling

A scaling on the $\vec{X}$ and $\vec{Y}$ axis of the image is applied:

Suppose

$$J(x,y) = I(x - x_0, y - y_0) \tag{34}$$

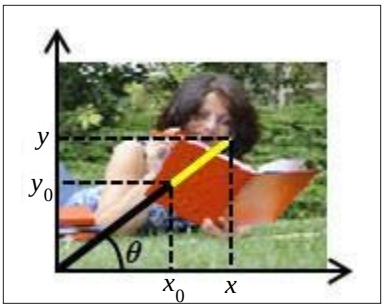

(35)

Figure 12. Scaling image on $\vec{X}$ and $\vec{Y}$ axis

The Radon transform of $J(x, y)$ is as follows:

$$DRT[J(x,y)] = R_1(\rho', \theta) = DRT[I(x - x_0, y - y_0)] \tag{35}$$

Where:

$$\rho' = (x - x_0)\cos\theta + (y - y_0)\sin\theta \tag{36}$$

$$\Rightarrow \rho' = x\cos\theta - x_0\cos\theta + y\sin\theta - y_0\sin\theta \tag{37}$$

$$\Rightarrow \rho' = \underbrace{x\cos\theta + y\sin\theta} - x_0\cos\theta - y_0\sin\theta \tag{38}$$

$$\Rightarrow \rho' = \rho - x_0\cos\theta - y_0\sin\theta \tag{39}$$

So:

$$DRT\,[J\,(x, y)] = R_1\,(\rho', \theta) = R\,(\rho - x_0 \cos\theta - y_0 \sin\theta\,,\, \theta) \tag{40}$$

Also, the error defined by $\Delta\rho = -x_0\cos\theta - y_0\sin\theta$ is lower than the value of ρ. Since $\Delta\rho$ cannot allow the projection of a pixel neighbor defined by its coordinates (ρ, θ), due to its size $\Delta\rho << \rho$ than the radon transformation depends only on the value of ρ.

4.1.3 Image rotation

Rotation attack is among the most popular kinds of geometrical attack on digital multimedia images. Supposing that $g\,(\rho, \theta)$ represents the polar coordinate of $I\,(x, y)$ and $J\,(\rho, \theta) = g\,(\rho, \theta - \varphi)$ with φ represents the angle of circular shifted, the Radon Transform has given the following results:

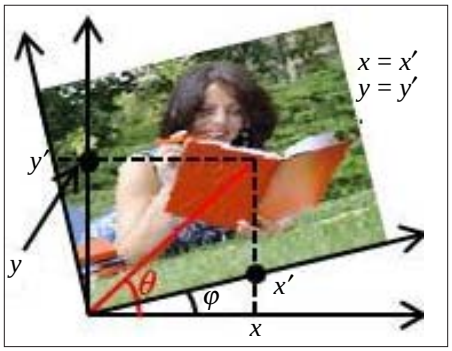

Figure 13. Circular shifted image by angle φ

$$DRT\,[J\,(\rho, \theta)] = DRT\,[g\,(\rho, \theta - \varphi)] = R_1\,(\rho', \theta')] = I\,(x\cos\theta\,\cos\varphi + x\sin\theta\,\sin\varphi\,, -y\cos\theta\,\sin\varphi + y\sin\theta\,\cos\varphi) \tag{41}$$

$$\Rightarrow R_1\,(\rho', \theta')] = I\,(x\cos(\theta - \varphi), y\sin(\theta - \varphi) \tag{42}$$

$$\Rightarrow R_1\,(\rho', \theta')] = R\,(\rho, \theta - \varphi) \tag{43}$$

$$\Rightarrow \rho' = \rho \text{ and } \theta' = \theta - \varphi \tag{44}$$

So:

$$DRT\,[J\,(p, \theta)] = R_1\,(\rho', \theta') = R\,(\rho, \theta - \varphi) \tag{45}$$

This relation shows that the radon transformation depends only on the value of $\theta - \varphi$ and its magnitude is constant. Consequently the projected pixel will change its location in the Radon field according to the angular rotation applied. This proves that this transform is invariant to angular rotations

4.1.4 Cropping rotation and scaling

In this section we test the invariance of the DRT if different asynchronous attacks are combined simultaneously such as rotation and scaling or cropping without changing the axis projection.

$$DRT\,[J\,(p, \theta)] = DRT\,[g\,(p, \theta - \varphi)] = R1\,(\rho', \theta')]$$

$$= I\,((x - x_0)\cos\theta\,\cos\varphi + (x - x_0)\sin\theta\,\sin\varphi\,, -(y - y_0)\cos\theta\,\sin\varphi + (y - y_0)\sin\theta\,\cos\varphi) \tag{46}$$

$$\Rightarrow R_1\,(\rho', \theta')] = R\,(\rho - x_0\cos(\theta - \varphi) - y_0\sin(\theta - \varphi), \theta - \varphi) \tag{47}$$

$$\Rightarrow \rho' = \rho - x_0\cos(\theta - \varphi) - y_0\sin(\theta - \varphi), \text{ and } \theta' = \theta - \varphi \tag{48}$$

So:

$$DRT\,[g\,(p, \theta - \varphi)] = R\,(\rho - x_0\cos(\theta - \varphi) - y_0\sin(\theta - \varphi), \theta - \varphi) \tag{49}$$

The error is defined by:

$$\Delta\rho = -x_0 \cos(\theta - \varphi) - y_0 \sin(\theta - \varphi) << \rho \tag{50}$$

Due to its feeble value, the error $\Delta\rho$ cannot change the original integer quantized coefficient in Radon field. So, the used coefficient to embed watermark do not change and the watermark is correctly recovered. As proved above, face to singular or composed geometric transform, the Radon transform offer an invariance to the transformed image.

4.2 Impact of the Radon transform on spatial imperceptibility of the watermarked image

The radon field is found to be a lossy domain. Once applied on the image matrix the inverse transform can engender a certain loss compared with the original image. This means that this transform is not conservative. This data loss can introduce some distortions to the processed image. We will prove in the following mathematical study that the non-conservatively of the radon transform disappear when dealing with image. In fact the distortion that affects the image due to the radon transform is under the perceptibility threshold defined by the Weber law. We noted the error between the original image and the Radon transformed and recovered image by $\underset{M_\theta N_\theta}{\varepsilon}$.

$$\underset{M\ N}{DRT}[I(x,y)] = \underset{M_\theta N_\theta}{R}(\rho - \theta) \tag{51}$$

$$\Rightarrow \underset{M_\theta N_\theta}{R}(\rho, \theta)\, O\left[\underset{M_\theta N_\theta}{R^{-1}} I(x,y)\right] = I(x,y) \neq I'(x,y) \tag{52}$$

Where
$$I(x,y) - I'(x,y) = \underset{M_\theta N_\theta}{\varepsilon}(x,y) \tag{53}$$

Or the Weber law impose that

$$\sum_{i=1}^{M}\sum_{j=1}^{N}\frac{I'(i,j) - I(i,j)}{I(i,j)} \leq \tau \text{ where } \tau \cong (2\% - 3\%) \tag{54}$$

Since the simulation results proved that $\underset{M_\theta N_\theta}{\varepsilon} < \underset{M_\theta N_\theta}{\tau}$

So, perceptually we can say that no visible changes are engendered by the application of the Radon transform:

$$\mathrm{I} = \mathrm{I}' \text{ and } \varepsilon \to 0 \tag{55}$$

The following figure illustrate an original and Radon transformed image followed by the positions of the distortions introduced by applying the radon transform and recovering the image by the inverse Radon transform.

Figure 15. Original image

Figure 16. IDRT image

In these section the robustness of the radon field against asynchronous attacks presented in table I is proved. In addition when dealing with image this transform is proved to be perceptually invariant.

5. Comparative Study

In order to prove the efficiency and high robustness of the proposed method, a comparison study is conducted with recent proposed approach resisting against geometric attacks. For this study we used lena color image. We compared the proposed method in this work with the recent proposed techniques in [8] and [9].

17. IDRT image Figure 17 Imperceptible Difference between original and recovered image by IDRT

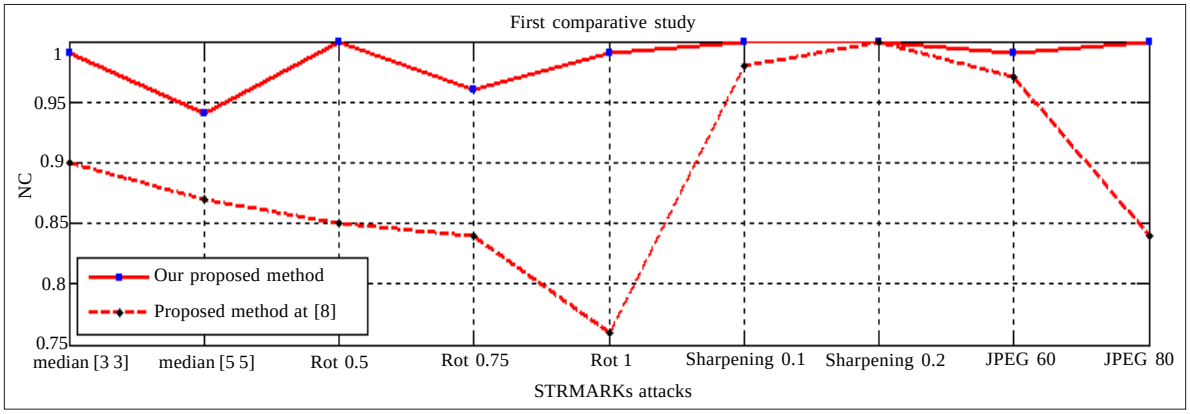

Figure 18. Comparative study between this proposed method and the recent proposed method at [8]

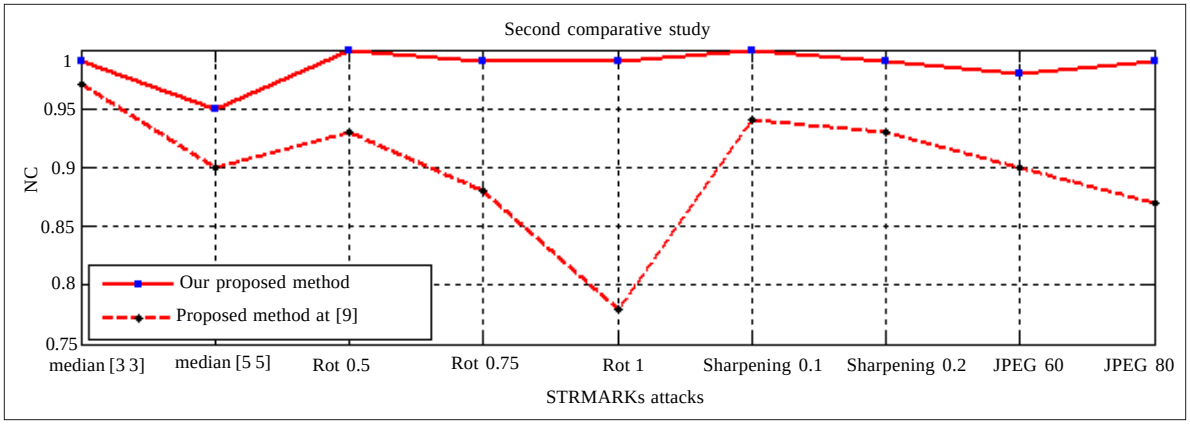

Figure 19. Comparative study between this proposed method and the recent proposed method at [9]

This study shows that the proposed approach in this work is more robust against different attack types than the recent proposed method in [8 and 9].

6. Conclusion

In this paper, a watermarking approach based on the Radon transform is presented. Embedded watermark is encrypted of the original one. Using encryption process ensures a good security of watermark and enhances the invisibility and robustness of watermark. The watermark is coded in selected coefficients exploiting specific mathematical characteristics of this domain. The proposed scheme presents high robustness especially against asynchronous attacks. This resistance against these geometric

attacks is proved mathematically. Equilibrium between watermarking constraints is achieved. Robustness and imperceptibility are respected and the embedded capacity is increased. A comparison study with recent proposed techniques robust against geometrical transformation also conducted. It proves the higher robustness of this proposed approach.

References

[1] Averbuch, A., Sedelnikov, I., Shkolnisky, Y. (2012). CT Reconstruction From Parallel and Fan-Beam Projections by a 2-D Discrete Radon Transform, *IEEE Transactions On Image Processing*, 21 (2).

[2] Channapragada, RSR., Mantha, AS., Munaga V.N.K. Prasad. (2012). Study Of Contemporary Digital Watermarking Techniques, *IJCSI International Journal of Computer Science Issues*, 9 (6, 1) 1694-0814.

[3] Gunjal, BL., Manthalkar, R.R. (2010). An Overview Of Transform Domain Robust Digital Image Watermarking Algorithms, *Journal of Emerging Trends in Computing and Information Sciences*, 2 (1) *CIS Journal*.

[4] Hussein, J. A. (2010). Spatial Domain Watermarking Scheme for Colored images based on log-average luminance, *Journal of Computing* 2 (1) 2151-9617.

[5] Lusson, F., Bailey, K., Leeney, M., Curran, K. (2013). A novelapproachtodigitalwatermarking,exploiting colour spaces, S*ignal Processing*, 93, 1268–1294.

[6] Simitopoulos, D., Koutsonano, D., Strintzis, M. G. (2002). Image watermarking resistant to geometric attacks using generalized radon transformations, *IEEE*, (DSP 2002 - 85).

[7] Simitopoulos, D., Koutsonanos, D. E., Strintzis. (2003). Robust Image Watermarking Based on Generalized Radon Transformations, *IEEE Transactions on Circuits and Systems for Video Technology*, 13 (8), August.

[8] Su, Q., Niu, Y., Liu, X., Yao, T. (2012). A novel blind digital watermarking algorithm for embedding color image into color image, *journal homepage*, Elsevier GmbH. *IJLEO*-52684, p. 6, 20.

[9] Vahedi, E, Zoroofi, RA., Shiva, M. (2012). Toward a new wavelet-based watermarking approach for color images using bio-inspired optimization principles, *Digital Signal Processing*, 22, p. 153–162.

[10] Xiao, B., FengMa, J., TaoCui, J. (2012). Combined blur, translation, scale and rotation invariant image recognition by Radon and pseudo-Fourier–Mellin transforms, *Pattern Recognition*, 45, p. 314–321.

[11] Zhu, H., Liu, M., Li, Y. (2010). The RST invariant digital image watermarking using Radon transforms and complex moments, *Digital Signal Processing*, 20, 1612–1628, Contents lists available at ScienceDirect.